doi:10.1017/S1431927621001033
Microsc. Microanal. 27 (Suppl 1), 2021

Magnetism and phonons in transmission electron microscopy

Jan Rusz[1], Paul Zeiger[1], Keenan Lyon[1], Alexander Edström[2], Axel Lubk[3] and Anders Bergman[1]

[1]Uppsala University, Uppsala, Sweden, [2]KTH Royal Institute of Technology, Sweden, United States, [3]IFW Dresden, Germany, United States

Recent dramatic improvements in the instrumentation have allowed for the detection of scattered electrons with energy resolutions well below 10 meV [1] while maintaining atomic spatial resolution [2]. Improved detectors [3] are approaching noise levels close to purely shot noise, allowing for the analysis of more and more subtle effects, such as detailed phonon band structures. Nowadays, monochromated electron energy loss spectroscopy (EELS) has made possible the distinction of isotope compositions and vibrational signatures of individual defects, such as impurity atoms [4] or stacking faults [5].

These significant achievements call for development of theoretical methods, versatile enough to take into account the experimental geometry (such as electron beam shape and direction) and electron beam propagation effects, capable of treating 2-dimensional and bulk samples with arbitrary atomic structures. Such methods should be also efficient enough for large structure models containing tens of thousands of atoms, allowing for a description of scattering on interfaces, various types of defects, or even isotope compositions.

We have developed a method with the overarching goal of satisfying these demands [6]. Non-equilibrium molecular dynamics calculations offer a route to avoid explicit calculation of individual phonon modes, which can be prohibitively expensive for large structure models. Thus, an evolution of the frozen phonon model leads to a frequency-resolved frozen phonon multislice method, a method largely preserving the flexibility and efficiency of frozen phonon multislice calculations, while also offering the spectroscopic dimension. We will present examples of vibrational EELS simulations of systems with defects at both the nanometer and atomic scale. Figure 1 shows nanometer scale contrast in vibrational EELS spectra simulated within a planar defect region, compared to a defect-free region.

Another frontier opened up by improved instrumentation is magnetism. Interaction of an electron beam with magnetic fields inside the sample is inherently weaker than the corresponding interaction with electric fields. Experimental work by Loudon [7] has revealed a minuscule magnetic Bragg peak in an antiferromagnetic NiO sample under the Neel temperature. While this experiment was challenging, increased sensitivity of instruments will make such experiments more easily accessible.

To describe the propagation of an electron beam through a magnetic sample, an extension of the classical multislice method is required. The recently developed Pauli multislice method [8] builds such a formalism starting from the Pauli equation instead of the Schrödinger equation. Using this method we have studied interaction of magnetism in samples with electron beams [8] and described an extension of the atomic scale differential phase contrast (DPC) method to magnetic materials [9]. Figure 2 shows a simulation of an atomic scale magnetic DPC experiment for FePt.

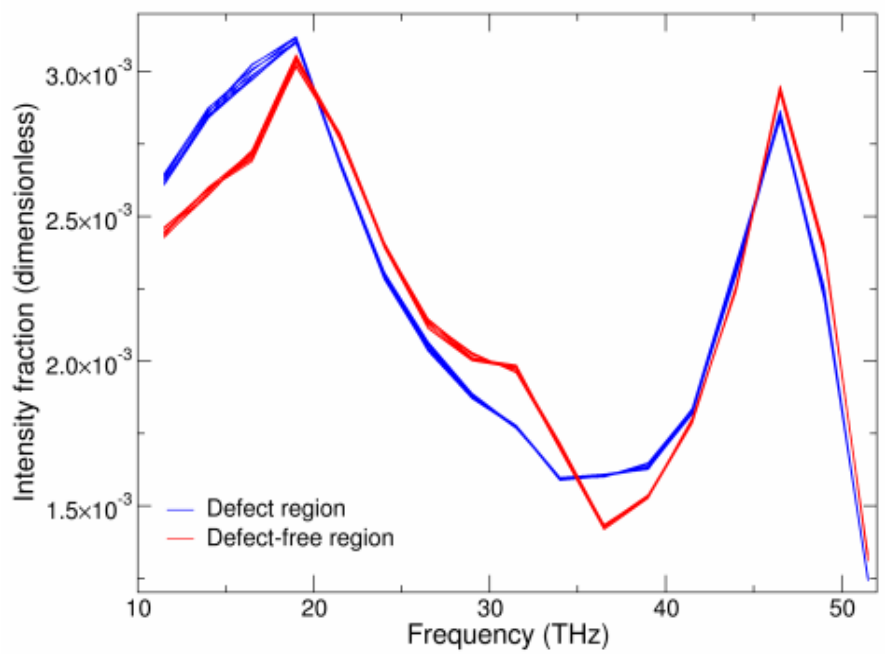

Figure 1. Simulation of vibrational spectra of a 15nm thick hexagonal BN sample with a planar defect. Red and blue curves represent vibrational EELS predicted for a 3 mrad semi-angle nano-beam and an off-axis detector with 25 mrad collection semi-angle within the region of the defect (blue curve) and within defect-free region (red curve).

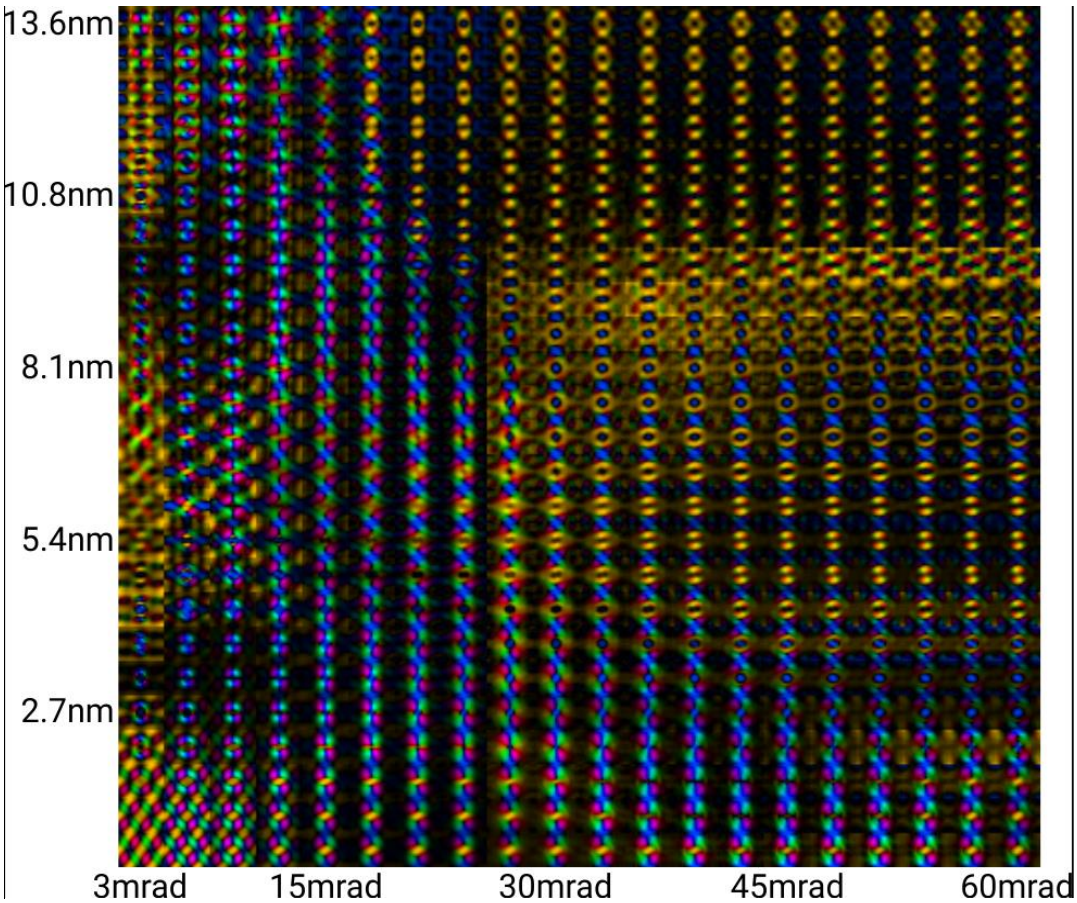

https://doi.org/10.1017/S1431927621001033 Published online by Cambridge University Press

Figure 2. Simulation of the microscopic magnetic fields detected by atomic scale magnetic differential phase contrast imaging in FePt as a function of sample thickness and collection semi-angle for a 100 kV electron beam. The magnetic moments of Fe are assumed to point along the x-axis, parallel with the c-axis of the FePt unit cell.

References

[1] O. Krivanek et al., Nature 514, 209 (2014).
[2] F. Hage et al., Phys. Rev. Lett. 122, 016103 (2019)
[3] B. Plotkin-Swing et al., Ultramic. 217, 113067 (2020).
[4] F. Hage et al., Science 367, 1124 (2020).
[5] X. Yan et al., Nature 589, 65 (2021).
[6] P. Zeiger and J. Rusz, Phys. Rev. Lett. 124, 025501 (2020).
[7] J. C. Loudon, Phys. Rev. Lett. 109, 267204 (2012).
[8] A. Edström, A. Lubk, J. Rusz, Phys. Rev. Lett. 116, 127203 (2016).
[9] A. Edström, A. Lubk, J. Rusz, Phys. Rev. B 99, 174428 (2019).

https://doi.org/10.1017/S1431927621001033 Published online by Cambridge University Press